Utilization of DC Chopper For Non-Conventional Energy Sources

Rahul Mishra[1], Javed Khan Bhutto[1], Sunil Kumar[2]

1Department of Electrical Engineering, MEC, Bikaner
2 Department of Electronics Engineering, Shoolini university, Solan
E-mail: rahulmishra24@gmail.com

Abstract: - The main aim of this paper is to computing and finding true solution of connecting various component of renewable energy sources like solar , wind, tidal geo thermal etc and get more efficiency lower cost and least losses.

A multi input and single out put DC chopper can be used to obtain well regulated output voltage from several power source such as solar wind tidal geo thermal etc. the energy provided by these source can be amalgamate and transfer in to the load. A theoretical idea of dc chopper are given here. Practical implementation also tested.

A method which has proved to be an asset when one is concerned with optimization problems is artificial immune system. Several other methods such as the likes of Ant Colony Optimization (ACO), Genetic programming (GP), Simulated Annealing (SA), and Particle Swarm Optimization (PSO), Genetic Algorithm (GA), have been used and tried, but none could give the results as fast and as accurately as Dc-DC converter.

By DC chopper technique used in computing to find true solution for source connection.

Key words:- Solar Energy, wind energy, DC-DC converter**.**

I. Introduction

Now a days resources of renewable energy ,such as wind turbines, photovoltaic arrays & fuel cells have been used for developing renewable electric power generation systems[1]-[3] .The multiple-input chopper shown in Figure 1(X), is useful for adding several energy sources whose power capacity are different to obtain well-regulated outputs voltage or current[4]-[7] . We can feed multi inputs of energy

sources in parallel using a coupled transformer. As shown in figure 3(y). Only 1energy source is allowed to transfer energy to the load at a time (i.e.E_1~E_N). These circuits for input-stages are designed in an "mode of n- inputs & single output operation" as shown in Fig. 1(y) to avoid power coupling effects. The current ratings for these input-stage circuits are higher with more complicated n- inputs & single

output control circuits. A multi input power supply system based on the current-fed full-bridge converter, shown in diagram. 2(x), is considered a better option for such applications[8]-[10] . In this we are using a phase-shift PWM control scheme, the energy from the different power sources can be simultaneously transferred into the load through a multi-winding transformer as shown in Fig. 2(y). Here, a large number of power switches and a complicated gating driver and controller are needed, hence its expansive and having large size for this conventional converter. , a multi-input chopper is presented for renewable energy systems shown in Fig.3(y). The proposed converter has the advantages of (1) It has simple configuration, (2)It has fewer components, (3) It has lower cost (4) It has higher efficiency. The design and operating principles will be explained in detail in the following sections, Is Spice simulations are given to confirm the theoretical analysis. The two-input laboratory prototype was implemented and tested to show the performance of the proposed converter.

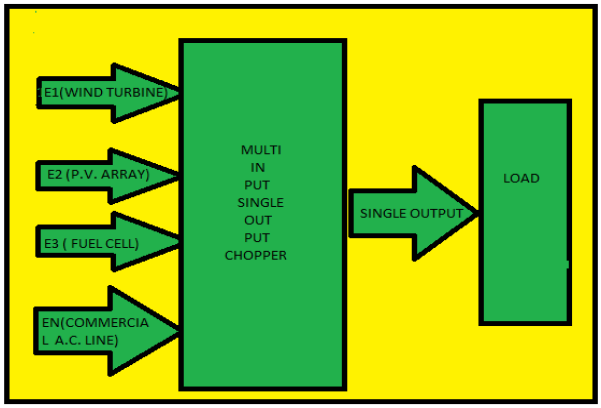

Fig1.1Multy input chopper for Non-conventional energy source

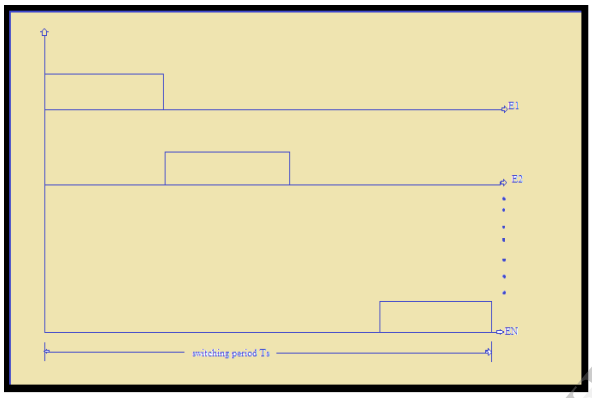

Fig 1.2 Input voltage signals applied to the input stage circuit.

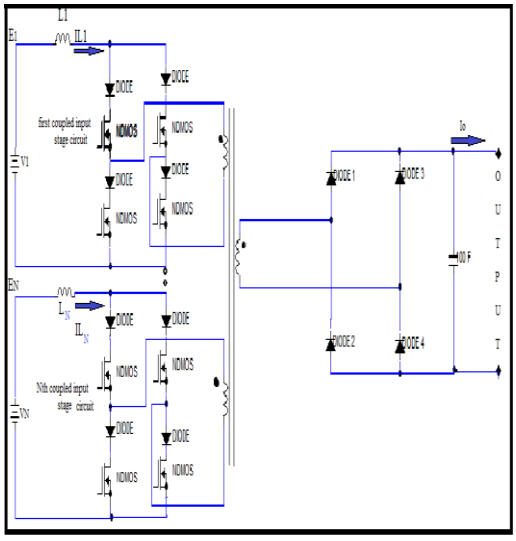

Fig.1. 3The Proposed Multiple-Input chopper

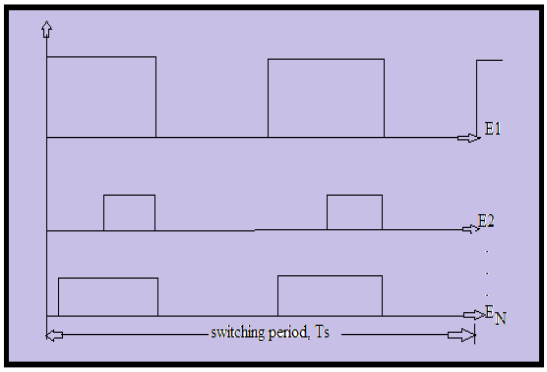

Fig 1.4 switching period

II. Operating Principle of the Proposed Converter

For analysis comfort ability, a simplified circuit diagram of the suggested chopper with v_{1}& v_{2} inputs is shown and discussed in Fig. 4(y). It is having the two current-fed input-stage circuits, coupled transformer, and a secondary bridge-rectifier. Each input-stage circuit consists of two, power switches and choke inductors L1 & L2. The duty ratio δ1 & δ2 (for the power switches Gs1 and Gs in the first input-stage circuit and for the power switches Gs3 and Gs4 in the second input-stage, respectively.) the circuit are regulated independently by two separated control loops. Both δ1 and δ2 exceed 0.5 to implement the overlapping operation. The proposed multi-input chopper is suitable for high-voltage output applications [8] due to the current-fed circuit topology being used that requires no output indictor.

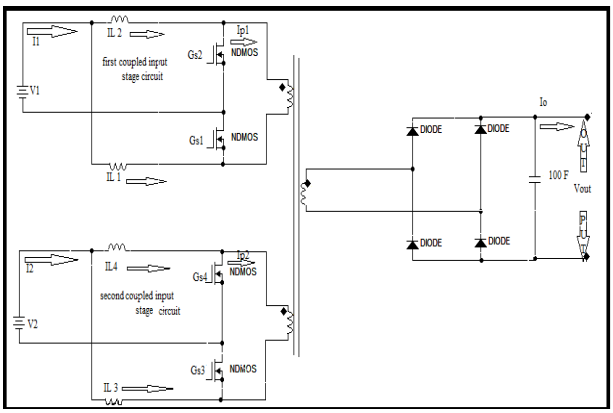

Fig2.1 The Circuit Diagram of the Proposed chopper with Two-Input

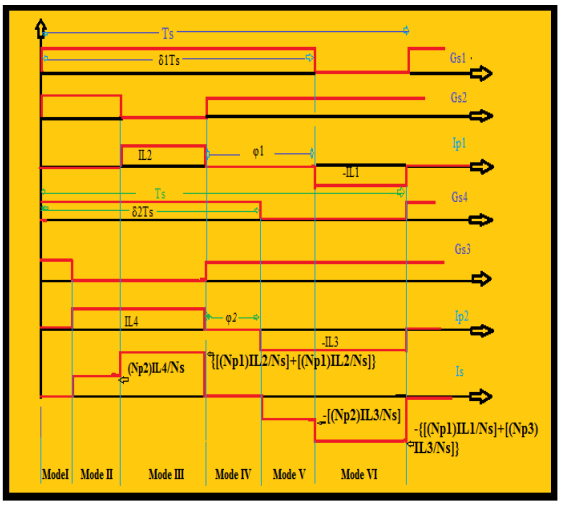

Fig 2.2 The un experimental Waveforms for One Switching Cycle

Here, the overlapping-times ϕ_1 and ϕ_2 can be given as follows.

$\phi_1 = (2\delta_1 - 1)T_s/2$……(1)

$\phi_2 = (2\delta_2 - 1)T_s/2$ ……(2)

There are 6 modes of switching within an operating cycle T_s. Now we will elaborate the equivalent circuits in Fig. 6. The working principle of the suggested chopper can be elaborated as follows.

Mode I (Gs**1,** Gs**2,** Gs**3, and** Gs**4 on):** During this operating mode ;Power switches Gs1~ Gs 4 are on. (2) The inductor currents, I_{L1} and I_{L2} will flow back towards the first voltage source, V1 ,through the path , Gs1and Gs2. (3)The inductor currents, I_{L3} and I_{L4} will flow back towards the second voltage source, V2 through the path Gs3& Gs4.(4) The remaining gathered energy in the leakage inductance of the second primary winding is also delivered to the load through the transformer and when , the gathered energy is released entirely, the trans- former secondary winding current will go to zero. (5)All the working diodes are off and the power to the load is provided only by the output capacitor C_o.

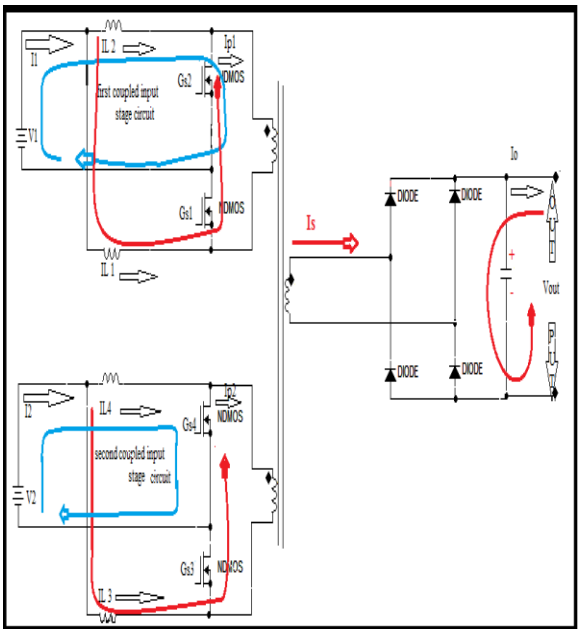

Fig 2.3 Mode I operation of chopper

(2)Mode II (Gs**1,** Gs**2 and** Gs**3 on;** Gs**4 off):** During this operating mode;

The power switches Q Gs1 and Gs2 are on. (2)Both of the inductor currents, I_{L1} and I_{L2} flow back to the first voltage source, V1 through Gs1 and Gs2.(3)The falling current in Gs4 occurs at zero voltage and there is no dissipation caused by Gs4 turning off. (4)The inductor current, I_{L3} flows through Gs3 back to the second voltage source, V2. (5) Only the inductor current, I_{L4} flows into the transformer primary winding. The energy from the second power source is transferred to the load through the rectifying diodes D1 and D4. The transformer secondary current, I_s satisfies Equation (3).

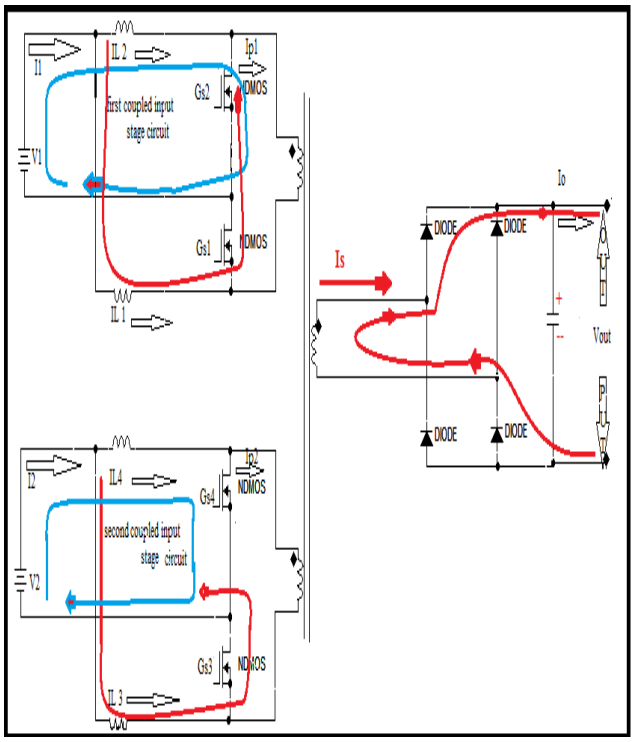

Fig 2.4 Mode II operation of chopper

$$I_s = \frac{N_{p2}}{N_s} I_{L4}, \qquad (3)$$

Mode III (Gs1 and Gs3 on; Gs2 and Gs4 off): in this mode;

(1)The falling current in Gs2 occurs at zero voltage and there is no dissipation caused by Gs2 turning off. (2)The inductor current, I_{L1} flows through Q1 back to the first voltage source, V1 and the inductor current, I_{L3} flows through Gs3 back to the second voltage source, V2. (3)The inductor current, I_{L2} flows into the first transformer primary winding and the inductor current, I_{L4} flows into the second transformer primary winding. (4)Thus, the transformer secondary current, I_s satisfies Equation (4). (5)The energy from the two power sources is transferred to the load through the rectifying diodes D1 and D4.

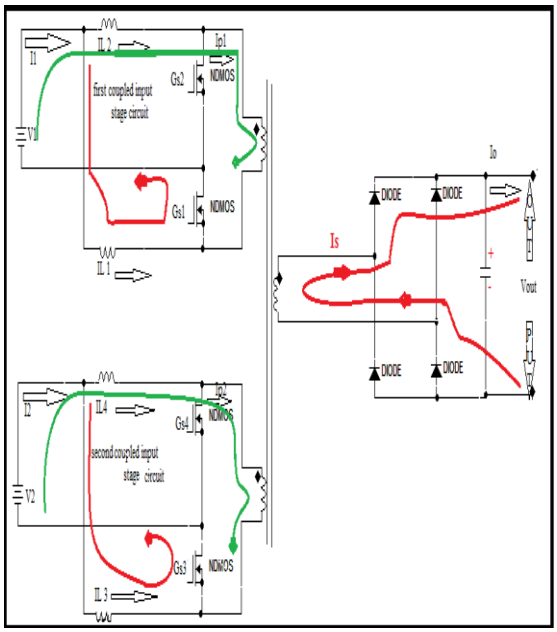

Fig 2.5 Mode III operation of chopper

$$I_s = \frac{N_{p1}}{N_s} I_{L2} + \frac{N_{p2}}{N_s} I_{L4}, \qquad (4)$$

Mode IV (Gs1, Gs2, Gs3, and Gs4 on): During this working mode;

(1)All power switches Gs1~Gs4 are on.(2)The inductor currents, I_{L1} and I_{L2} flow back to the first voltage source, V1 through Gs1 and Gs2.(3) The inductor currents, I_{L3} and I_{L4} flow back to the second voltage source, V2 through Q3 and Gs4. (2)The rising currents in Gs2 and Gs4 occur at zero voltage and there is no dissipation caused by Gs2 and Gs4 turning on. (3)The surviving energy in the leakage inductance of the second primary winding is also delivered to the load through the transformer. (4)When the surviving energy is released completely, the transformer secondary winding current will collapse to zero. All the rectifying diodes are off and the load power is provided alone by the output capacitor C_o.

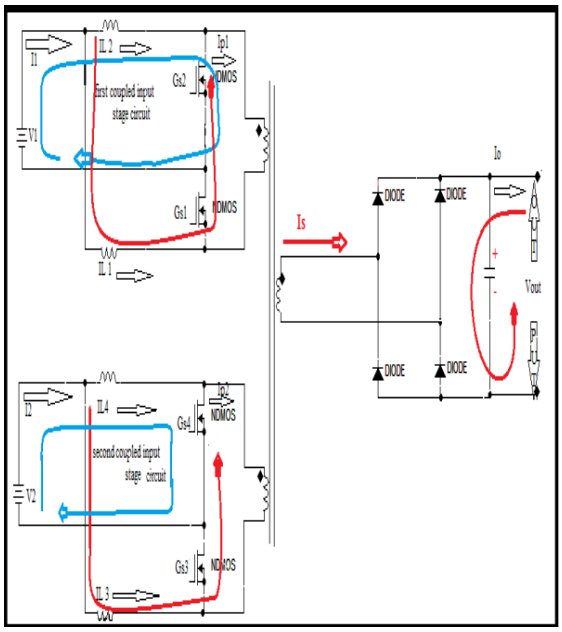

Fig 2.6 Mode IV operation of chopper

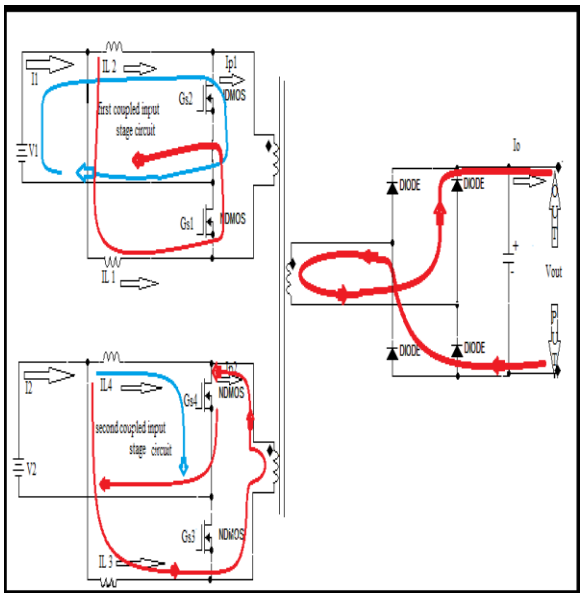

Fig 2.7Mode V operation of chopper

Mode V (Gs1, Gs2 and Gs4 on; Gs3 off): During this mode;

(1) The power switch Gs3 is off. (2) The falling current in Gs3 occurs at zero voltage and there is no dissipation caused by Gs3 turning off. (3)The inductor current, I_{L3} flows through the transformer primary winding. Both of the inductor currents, I_{L1} and I_{L2} still flow back to the first voltage source, V1 through Gs1 and Gs2. The inductor current, I_{L4} flows through Gs4 back to the second voltage source, V2. (4)The energy transferred to the load through the rectifying diodes D2 and D3 is from the second power source. The transformer secondary current, I_s satisfies Equation (5)

$$I_s = -\frac{N_{p2}}{N_s} I_{L3}, \qquad (5)$$

Mode VI (Gs2 and Gs4 on; Gs1 and Gs3 off): During this mode:

The falling current in Gs1 occurs at zero voltage and there is no dissipation caused by Gs1 turning off. (2)The inductor current, I_{L2} flows through Gs2 back to the first voltage source, V1 and the inductor current, I_{L4} flows through Gs4 back to the second voltage source, V2.(**3**)he inductor current, I_{L1} flows through the first transformer primary winding and the inductor current, I_{L3} flows through the second transformer primary winding. (4)Thus, the transformer secondary current, I_s satisfies Equation (6). The energy from the two power sources is transferred to the load through the rectifying diodes D2 and D3.

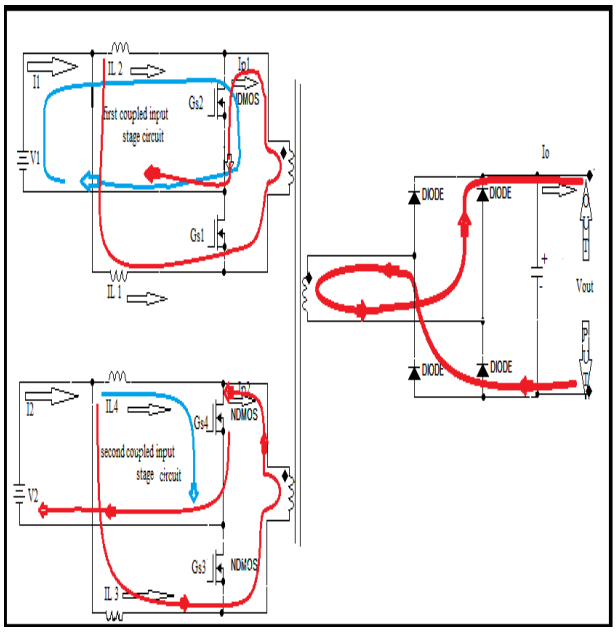

Fig 2.8Mode VI operation of chopper

$$I_s = -(\frac{N_{p1}}{N_s} I_{L1} + \frac{N_{p2}}{N_s} I_{L3}), \qquad (6)$$

The circuit will then follow the Mode I after completing one operating cycle T_s There is no dissipation caused by Gs1 and Gs3 turning on. The leakage inductances of the first and second primary windings provide their grabbed energy to the load through the transformer. When the surviving energy is released completely, the transformer secondary winding

III. Steady-State Analysis

Consider that the output capacitor C_o is large enough so that the voltage ripple on it is negligible. The voltage transfer ratio VTR of the suggested multiple-input chopper can be derived from the volt-second balance condition across the choke inductors and given by Equations (7) and (8).

$$VTR_1 = \frac{V_o}{V_1} = \frac{N_s}{N_{p1}} \frac{1}{1-\delta_1}, \qquad (7)$$

$$VTR_2 = \frac{V_o}{V_2} = \frac{N_s}{N_{p2}} \frac{1}{1-\delta_2}, \qquad (8)$$

$$V_{Q1,Q2} = \frac{N_{p1}}{N_s} V_o = \frac{V_1}{1-\delta_1}, \qquad (9)$$

$$V_{Q3,Q4} = \frac{N_{p2}}{N_s} V_o = \frac{V_2}{1-\delta_2}, \qquad (10)$$

$$I_{Q1,Q2} = I_{L1} + I_{L2} = I_1, \qquad (11)$$

$$I_{Q3,Q4} = I_{L3} + I_{L4} = I_2, \qquad (12)$$

From Equations (11) and (13), it is clear that the power switches subject only one source current and not twice as do the conventional two-switch circuit topologies such as push-pull converter or half-bridge converter. For the low-voltage energy source such as fuel cells, this is a very important merit. As explained above, all switches have negligible dissipation as they have the transformer leakage inductance in series and hence turn on at zero voltage. The zero voltage-switching condition of the power switches can be derived as follows.

$$L_{l1} \geq \frac{2V_o t_{r(max)}}{I_1} \frac{N_{p1}}{N_s}, \qquad (13)$$

$$L_{l2} \geq \frac{2V_o t_{r(max)}}{I_2} \frac{N_{p2}}{N_s}, \qquad (14)$$

where L_{l1} and L_{l2} are the leakage inductances of the first and the second primary windings respectively, and t_r =the maximum rise time of the switch current. The inductances of L_1~L_4 can be determined by the requirements of the inductor current ripples as follows:

$$L_1 = L_2 \geq \frac{2\delta V_1}{\Delta I_L(\%) I_1 f_s}, \qquad (15)$$

And equation no.(16) can be written as

$$L_3 = L_4 \geq \frac{2\delta V_2}{\Delta I_L(\%) I_2 f_s}, \qquad (16)$$

where f_s = the switching frequency of the power switches, $\Delta I_L(\%)$ = the percentage ripple current on the choke inductors L_1~L_4. The equivalent circuit of the input-stage circuit is shown in Fig.7(x). V_s and I_s represents the source voltages (V_1, V_2) and source current (I_1, I_2) respectively. $I_{L,I}$ is the upper inductor current (I_{L2}, I_{L4}) and $I_{L,j}$ is the lower inductor current (I_{L1}, I_{L3}).

Assuming the transformer turn ratio is n, the voltages V_i' and V_j' may be 0 or (V_o/n) for different switching modes. From the theoretical o/p waveforms shown in Fig. 7(y), the ripple cancellation on source current can be observed. This produces relatively ripple-free source current that is desired for the low voltage renewable energy sources such as fuel cells, photovoltaic arrays etc. From the energy conservation relationship, the output power P_o is the sum of the two sources of power P_1 and P_2. Thus, the following Equations must be obeyed.

$$V_o I_o = V_1 I_1 + V_2 I_2 \qquad (17)$$

$$I_o = (1-\delta_1)\frac{N_{p1}}{N_s} I_1 + (1-\delta_2)\frac{N_{p2}}{N_s} I_2, \qquad (18)$$

It is necessary to provide a feedback loop to regulate the output voltage and two current control loops are also needed to control the source current and power by each power source.

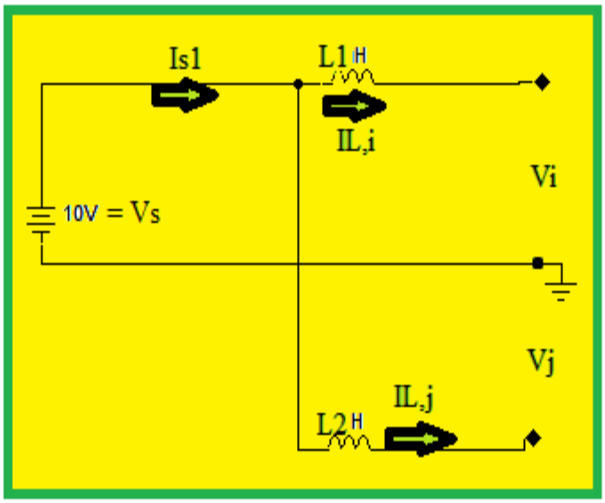

Fig.3.1The Equivalent Circuit

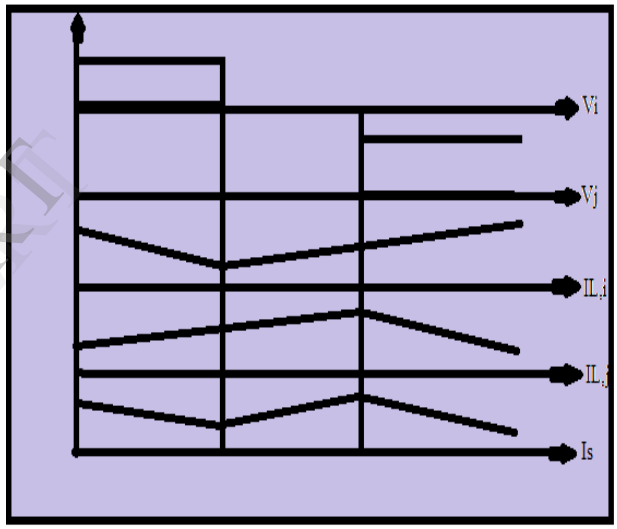

Fig 3.2Theoretical Waveforms of the Input-Stage Circuit

IV. Design Example of the Proposed Converter

To verify the feasibility of the proposed scheme, a lab prototype with following requirements was designed and tested. The design considerations for the key components will be explained in this section.

(1)Source voltage: V1=12VDC, V2=24VDC

(2)Source current: I1= 4A, I2= 6A

(3)Output voltage: Vo = 192VDC

(4) Output current: Io=1A

(5)Switching frequency: fs = 100kHz

A. Power Switches

These voltage and current ratings for the power switches can be calculated using Equations (9) to (12) as follows:

$$V_{Q1,Q2} = \frac{V_1}{1-\delta_1} = \frac{12}{1-0.6} = 30V\,, \quad (19)$$

$$V_{Q3,Q4} = \frac{V_2}{1-\delta_2} = \frac{24}{1-0.6} = 60V\,, \quad (20)$$

$$I_{Q1,Q2} = I_1 = 4A\,, \quad (21)$$

$$I_{Q3,Q4} = I_2 = 6A\,, \quad (22)$$

(B). Transformer

Design From the output voltage specification, the transformer turn ratios can be determined using Equations (7) and (8).

$$n_1 = \frac{N_s}{N_{p1}} = (1-\delta_1)\frac{V_o}{V_1} = (1-0.6)\frac{192}{12} = 6.4\,, \quad (23)$$

$$n_2 = \frac{N_s}{N_{p2}} = (1-\delta_2)\frac{V_o}{V_2} = (1-0.6)\frac{192}{24} = 3.2\,, \quad (24)$$

Equations (13) and (14) must be satisfied such that the zero-voltage-switching of the power switches can be achieved. Thus, the leakage inductances of the transformer first and second primary windings can be determined as follows.

$$L_{l1} \geq \frac{2V_o t_{r(max)}}{I_1}\frac{N_{p1}}{N_s} = 3\mu H\,, \quad (25)$$

$$L_{l2} \geq \frac{2V_o t_{r(max)}}{I_2}\frac{N_{p2}}{N_s} = 4\mu H\,, \quad (26)$$

(C.) Choke Inductors

Let the peak-to-peak current ripples be 30 percent of the inductor currents under full power. The inductance of the choke inductors L_1~L_4 can be determined using Equations (15) and (16) as follows.

$$L_1 = L_2 \geq \frac{2\delta V_1}{\Delta I_L(\%) I_1 f_s} = \frac{2\times 0.6\times 12}{0.3\times 4\times 100k} = 1.2mH\,, (27)$$

$$L_3 = L_4 \geq \frac{2\delta V_2}{\Delta I_L(\%) I_2 f_s} = \frac{2\times 0.6\times 24}{0.3\times 6\times 100k} = 1.6mH\,, (28)$$

Because of the ripple cancellation on the source current, a larger ripple current in choke inductors can be allowed in practical applications. Thus, the inductance and the size of these choke inductors might be smaller. D. Output Capa -citor The output capacitor must be large enough to provide the load power during Mode III and Mode VI without the voltage across it decreasing too much. The output capacitance can be then determined using Equation (27).

$$C_o \geq \frac{I_{o,max}\times T_s}{\Delta V_o} = \frac{1\times 10\mu}{0.001\times 192} \approx 52uF\,, \quad (29)$$

consider C_o=199.9µF.

VI. Conclusion

A multiple-input chopper for Non convensional energy systems was given in this paper. This chopper has various advantages as given ahead (1) very simple configuration, (2) fewer components, (3) lower cost and (4) higher efficiency. The working principles and design considerations were studied and explained in detail. Simulation results from the suggested circuit were given to verify the theoretical analysis. This experiment was implemented & tested with the satisfactory results in lab.

References

[1] M. Park, M. Michihira, and K. Matsuura, “A Novel MPPT Control Method using Optimal Voltage of PV with Secondary Phase-Shift PWM Control DC-AC Converter,” International Conference on Electric Power Engineering, Aug. 1999, pp. 269.

[2] F. Z. Peng, H. Li, G. J. Su, and J. S. Lawler, “A New ZVS Bidirectional DC-DC Converter for Fuel Cell and Battery Application,” IEEE Transactions on Power Electronics, Vol. 19, Jan 2004, pp. 54–65.

[3] K. Wang, C. Y. Lin, L. Zhu, D. Qu, F. C. Lee, and J. S. Lai, “Bi-directional DC to DC Converters for Fuel Cell Systems,” PET’98, pp. 47-51.

[4] G. J. Su, F. Z. Peng, and D. J. Adams, “Experimental Evaluation of a Soft-Switching DC-DC Converter for Fuel Cell Applications,” PET’02, pp. 39-44.

[5] H. Matsuo, Wenzhong Lin; F. Kurokawa, T. Shigemizu, and N. Watanabe, ”Characteristics of the Multiple-Input DC-DC Converter,” IEEE Transactions on Industrial Electronics, Vol. 51, June 2004, pp. 625-631.

[6] B. G. Dobbs, and P. L. Chapman, “A Multiple-Input DC-DC Converter Topology” IEEE Power Electronics Letters, Vol. 1, March 2003, pp. 6-9.

[7] H. Matsuo, K. Kobayashi, Y. Sekine, M. Asano, and Lin Wenzhong, “Novel Solar Cell Power Supply System using the Multiple-Input DC-DC Converter,” IEEE INTELEC, Oct. 1998, pp. 797-802.

[8] Y. M. Chen, Y. C. Liu, and F. Y. Wu, “Multi-Input DC/DC Converter Based on the Multiwinding Transformer for Renewable Energy Applications,” IEEE Transactions on Industry Applications, Vol. 38, July-Aug. 2002, pp. 1096-1104.

[9] Y. M. Chen, Y. C. Liu, and F. Y. Wu, “Multi-Input DC/DC Converter with Ripple-Free Input Currents,” IEEE PESC, Vol. 2, June 2002, pp. 796-802.

[10] Y. M. Chen, Y. C. Liu, F. Y. Wu, and T. F. Wu, “Multi-Input DC/DC Converter Based on the Flux Additivity” IEEE IAS, Vol. 3, Oct. 2001, pp. 1866-1873.